# Zeta-Based Universal Converter with Zero-Current Switching

Mojtaba Salehi

Department of Electrical and Computer Engineering

Northeastern University

Boston, MA, USA

salehi.mo@northeastern.edu

Mahshid Amirabadi

Department of Electrical and Computer Engineering

Northeastern University

Boston, MA, USA

m.amirabadi@northeastern.edu

Abstract—AC-link universal converters have emerged as promising topologies for efficient power conversion between various sources and loads. These converters offer enhanced reliability by replacing bulky electrolytic capacitors, which have a shorter lifetime compared to other power electronic components, with small and durable film capacitors. By doing so, the overall lifetime of the converter would be significantly extended. Additionally, AC-link converters achieve high-power density by utilizing compact high-frequency transformers when isolation is required, eliminating the need for large and heavy low-frequency transformers.

This paper introduces a new soft-switching Zeta-based universal converter capable of stepping up and down the voltage in a wide range. Building upon the operating principles of the Zeta DC-DC converter, the proposed converter extends its applications to inverters, rectifiers, and AC-AC converters. In this converter, an inductor and a capacitor are responsible for transferring the power from input to output. Another small inductor is employed in series with the link capacitor to allow all switches to have zero-current switching, resulting in improved efficiency. In isolated configurations, the leakage inductance of the transformer can be used for this purpose. Compared to conventional Ćuk-based universal converters, this topology employs a capacitor with a lower voltage rating. The performance of the proposed structure is verified through simulation and experimental results in this paper.

Keywords—ac-ac converter, high-frequency ac link, inverter, rectifier, soft-switching, universal converter, zero current switching (ZCS), Zeta converter, Ćuk converter.

#### I. INTRODUCTION

Due to the increasing energy consumption and the diversity of electrical loads and sources over the past few years, demand for efficient and reliable universal converters capable of transferring power from various sources to different kinds of loads is emerging. Employing conventional DC-link power converters may cause reliability concerns due to frequent failures and the short lifespan of electrolytic capacitors, especially at high temperatures [1]-[3]. Another drawback of traditional DC-link converters is the requirement for bulky low-frequency transformers to provide galvanic isolation. In response to these challenges, AC-link universal converters like Buck-boost-based and Ćuk-based converters have been introduced in [4]-[8], as potential solutions.

By extending the operation of DC-DC Buck-Boost converters, a family of AC-link universal converters can be

This material is based upon work supported by the National Science Foundation under Grant No. 2047213.

derived, serving as three-phase inverters, rectifiers, and AC-AC converters. Unlike conventional DC-link converters, a Buck-Boost-based universal converter uses an inductor, placed in parallel with input and output switch bridges, instead of an electrolytic capacitor at the link to transfer power from the input to the output. To reduce the size of the inductor, a high current ripple for the inductor can be allowed [4]. By integrating a small capacitor in parallel with the link inductor, soft-switching can be achieved, minimizing switching losses and enabling zero voltage turn-on and soft turn-off for all switches [5]. However, the main problem with this topology is the high link peak current, which leads to increased conduction losses and the current stress of the switches. To reduce address these problems, a soft-switching series Buck-Boost-based universal converter, which extends the operation of DC-DC noninverting buck-boost converter to inverters, rectifiers, and AC-AC converters, is introduced in [6].

Efficiency is a constant challenge in Buck-Boost-based converters. However, Ćuk-based universal converters can serve as an alternative solution by using a small series film capacitor as the energy-transferring element [7]. To achieve soft switching, a small series inductor is added to the link which enables zero current turn-off and a soft turn-on for all switches [8]. Despite this advantage, Ćuk-based universal converters are faced with the drawback of high link peak voltage.

To address the aforementioned challenge, a soft-switching Zeta/SEPIC inverter/rectifier with a lower link peak voltage was proposed in [9]. In these converters, all switches benefit from zero current turn-off and soft turn-on, minimizing switching losses. Furthermore, in [10] and [11], hard-switching and soft-switching Zeta-based rectifiers and Zeta-based AC-AC converters with a lower capacitor link peak voltage were proposed. The proposed soft-switching method in [11] allows the output side diodes to benefit from zero current turn-off and soft turn-on. Simultaneously, the input side switches benefit from zero voltage turn-on and soft turn-off.

This paper introduces another soft-switching method for the Zeta-based universal converter, which can be configured as a rectifier, an AC-AC converter, and an inverter. In the proposed converter, a small series inductor is added in series with the link capacitor, accompanied by a proper control method, enabling all switches to benefit from zero current turn-off and soft turn-on. By implementing this topology, the need for bulky electrolytic capacitors is eliminated, and the converter achieves

higher power density by utilizing lightweight high-frequency transformers instead of heavy line-frequency ones.

This paper is organized as follows: The topologies and operating principles are introduced in Section II. In Section III, simulation and experimental results are presented to verify the performance of the proposed system. And finally, in section IV, a summary and a conclusion are provided.

### II. OPERATING PRINCIPLES

This section discusses the operating principles and control strategies of the proposed soft-switching Zeta-based rectifier and AC-AC converter, respectively in parts (A) and (B). The soft-switching technique employed in both cases ensures a zero current turn-off and a soft turn-on for all switch transitions.

## A. Three-phase Zeta Rectifier

Fig. 1 shows the isolated soft-switching Zeta rectifier. The power transfer from the input to the output is facilitated by the input inductor ( $L_{in}$ ) and the link capacitors ( $C_1$  and  $C_2$ ). Additionally, a small resonating inductor ( $L_{resonance}$ ) is connected in series with each link capacitor to provide the resonating modes. It is worth noting that the isolation is provided with a high-frequency transformer (HFT) when it is required, and the transformer is optional. In non-isolated topologies, only one capacitor is necessary instead of  $C_1$  and  $C_2$ . To clarify the system behavior, Fig. 2 shows the link voltage, link current, and input inductor voltage waveforms during different modes.

During each cycle, two main power transfer cases occur in the proposed Zeta-based rectifier. In the first case, power is transferred from the input inductor ( $L_{\rm in}$ ) to the link capacitor ( $C_{\rm link}$ ), resulting in the charging of the link capacitor and the discharging of the input inductor. In the second case, the input inductor is charged from the input source while the link capacitor discharges to the output load. The detailed behavior of the proposed non-isolated topology during different operating modes is illustrated in Fig. 3. In this figure it is assumed  $I_A^{ref}$ , the reference current of phase A, is positive and has the maximum absolute value among the three-phase

currents. The reference currents of phases B  $(I_B^{ref})$  and C  $(I_C^{ref})$ , are negative and the absolute value of  $I_C^{ref}$  is smaller than  $I_B^{ref}$ . It is obvious that based on the absolute values of input currents, different switching patterns need to be selected.

Throughout each cycle, there are four distinct operating modes for the output side and three operating modes for the input side. The initial mode, characterized by the absence of switch activation, allows the input inductor current (I<sub>in</sub>) to charge the link capacitor via the DC-side antiparallel diode (Fig. 3(a)). As the link capacitor voltage reaches its peak, the appropriate switches are triggered, marking the start of the second mode. Mode 2 contains a resonating behavior for the link capacitor alongside a charging mode for the input inductor. It should be noted that during mode 1, the unfiltered input currents and the unfiltered output voltage remain at zero.

Mode 2 of the converter activates switches  $Q_1$  and  $Q_5$  to charge the input inductor with the highest line-to-line voltage  $(V_{AB})$ . Simultaneously, the link capacitor and its series inductor enter a resonating state through the short circuit provided by the DC side diode until the link current reaches  $-|I_o|$  to turn it off under ZCS condition (Fig. 3(b)). Once the diode turns off, the link capacitor discharging mode starts.

The first input inductor charging mode is ended when  $I_B^{average}$  meets  $I_B^{ref}$ , and switch  $Q_5$  is turned off. It is important to note that the unfiltered output voltage during this mode is equal to  $V_{AB}+V_{link}$ . Subsequently, switch  $Q_6$  can be activated to charge the input inductor with  $V_{AC}$  in the second charging mode (Fig. 3(d)). The unfiltered output voltage would be equal to  $V_{AC}+V_{link}$ . As the link voltage reaches  $-V_{AC}$ , switch  $Q_{dc}$  turns on to start the last resonating mode (output mode 4).

In output mode 4, the link current initially flows in the negative direction through  $Q_{\rm dc}$ . Once the link current reaches zero,  $Q_{\rm dc}$  stops conduction under ZCS conditions, allowing its antiparallel diode to conduct the positive link current. This mode continues until the link current aligns with the input inductor current to turn off  $Q_1$  and  $Q_6$  under ZCS. It is noteworthy that the duration of the resonating modes is considerably shorter than the power-transferring modes.

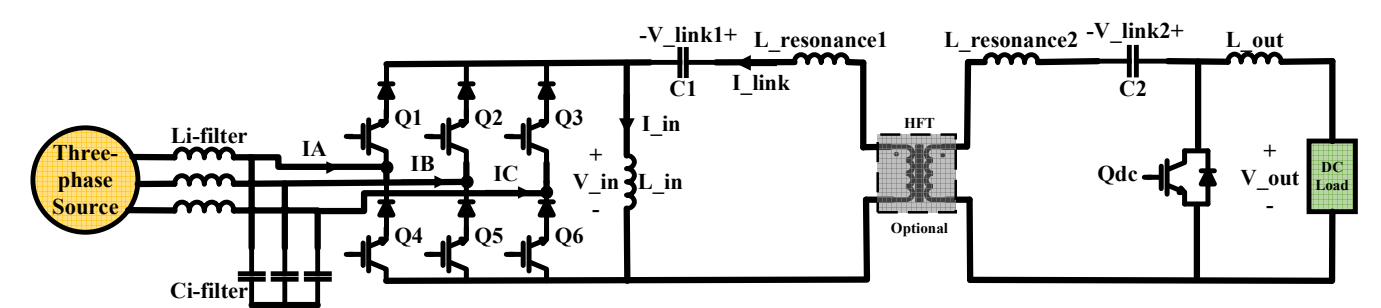


Fig. 1. Isolated soft-switching Zeta-based three-phase rectifier.

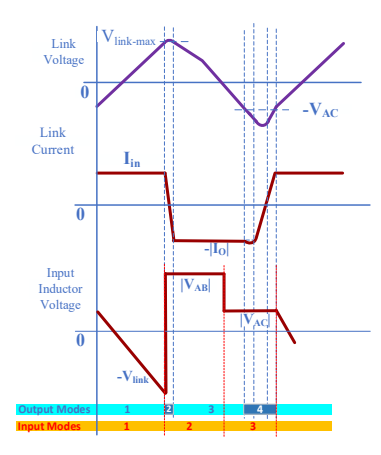


Fig. 2. Voltage and current waveforms of the link capacitor and input inductor in the Zeta-based rectifier.

# B. Zeta-based Three-phase AC-AC Converter

The isolated soft-switching three-phase Zeta-based AC-AC converter is illustrated in Fig. 4. To gain a better understanding of the system behavior, the link voltage and current are depicted in Fig. 5. Furthermore, the behavior of the proposed soft-switching converter for each operating mode is shown in Fig. 6.

Within each cycle, there are six operating modes dedicated to the output power transfer and resonances, in addition to three modes for the input power transfer. The first input and output mode as well as input modes 2 and 3 are similar to those of the Zeta rectifier discussed in the preceding section (Figs. 6(a), (b), and (c)).

In Figs. 5 and 6, for the link capacitor discharging modes, it is assumed that  $V_{ABO}^{ref}$ , the voltage reference of phase pair AB for the three-phase load, is positive and has the highest absolute value among the three-phase output line-to-line voltages. Conversely, the other line-to-line reference voltages,  $V_{BCO}^{ref}$  and  $V_{CAO}^{ref}$ , are negative, with the absolute value of  $V_{CAO}^{ref}$  being smaller than  $V_{BCO}^{ref}$ . The polarities and magnitudes of the output line-to-line voltages dictate the appropriate switching operations for each cycle at the output side. Regarding the input

inductor charging modes, similar to the discussion for the rectifier case, the assumption is made that  $I_A^{ref}$  is positive and has the maximum absolute value. On the other hand,  $I_B^{ref}$  and  $I_C^{ref}$  are negative, with the absolute value of  $I_C^{ref}$  being smaller than  $I_B^{ref}$ .

In mode 1, all switches are in the off state, allowing the power to be transferred from the input inductor  $(L_{in})$  to the link capacitor  $(C_{link})$  through the output side antiparallel diodes. Once the link capacitor is fully charged, the appropriate switches are activated to finish this operating mode. After mode 1, the first resonating mode (output mode 2) and the first input inductor charging mode (input mode 2) start simultaneously.

During the first resonating mode, switches  $Q_7$  and  $Q_{11}$  are kept on establishing a resonating path for the link capacitor and its corresponding series inductor. As a result, the link current decreases gradually leading to turn of the antiparallel diode of  $Q_{12}$  off under ZCS (Fig. 6(d)). This mode continues until the link current reaches a value equal to  $-|I_{Bo}|$  (the second highest load current).

In the first capacitor discharging mode, the energy stored in the link capacitor is transferred to the three-phase load through the switches  $Q_7$ ,  $Q_{11}$ , and the antiparallel diode of  $Q_9$ . When  $V_{BCo}^{\ average}$  meets its reference value, this mode ends, and another resonating mode starts.

During output mode 4, which is a resonating mode, both  $Q_{12}$  and the antiparallel diode of  $Q_9$  are conducting, creating a resonance between  $L_{\rm resonance}$  and  $C_{\rm link}$  to help turn the diode off under ZCS (Fig. 6(f)). As a result, the link current gradually becomes more negative until it reaches - $|I_{\rm Ao}|$  (the highest load current).

The last discharging mode is responsible for transferring the remaining energy stored in the link capacitor to the load with the load current  $|I_{Ao}|$ , which flows through switches  $Q_7,\,Q_{11},$  and  $Q_{12}$  (Fig. 6(g)). The link voltage can become negative during the discharging modes with no issue. As long as  $V_{\rm in}+V_{\rm link}$  is positive, the antiparallel diodes of the output switches will not become undesirably forward biased. Once the link voltage reaches - $V_{AC}$ , switch  $Q_9$  turns on to start the last resonating mode

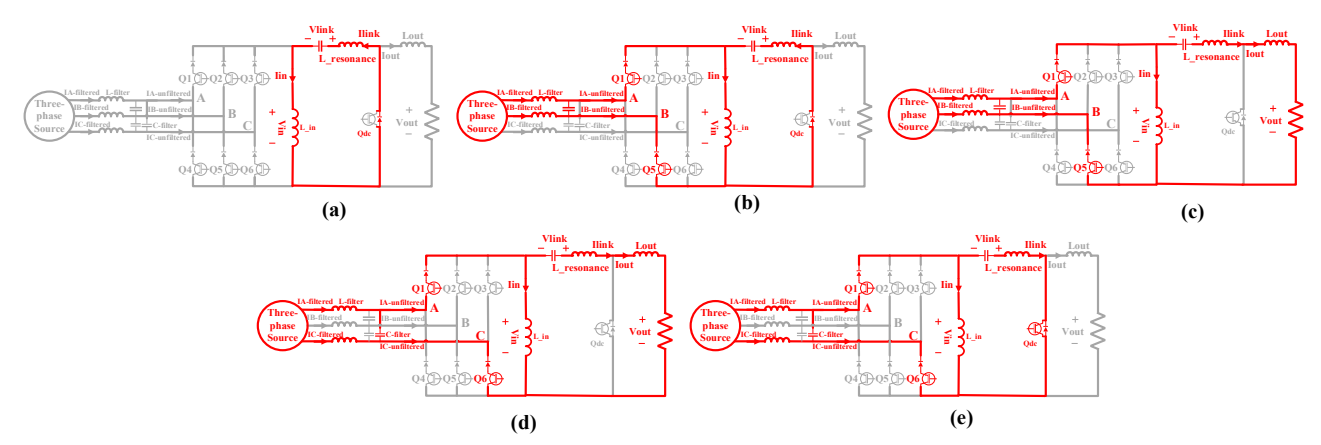


Fig. 3. Behavior of the non-isolated soft-switching three-phase Zeta rectifier during: (a) mode 1, (b) output mode 2 and input mode 2 (first charging mode), (c) output mode 3, (d) output mode 3 and input mode 3 (second charging mode), (e) output mode 4.

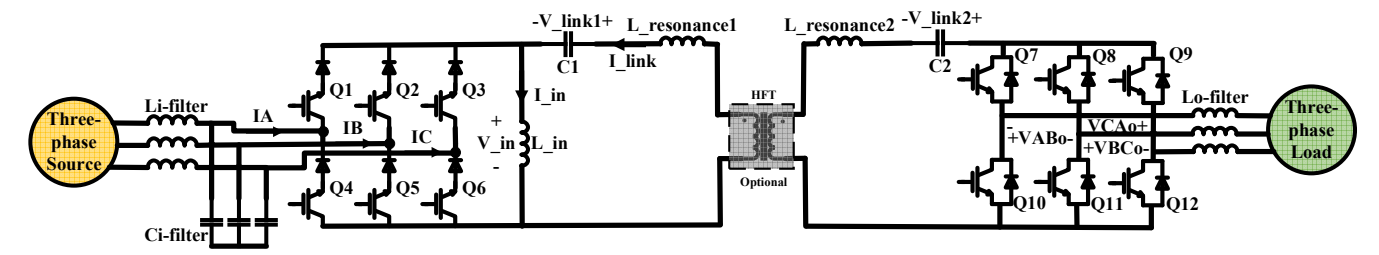


Fig. 4. Isolated soft-switching three-phase Zeta-based AC-AC converter.

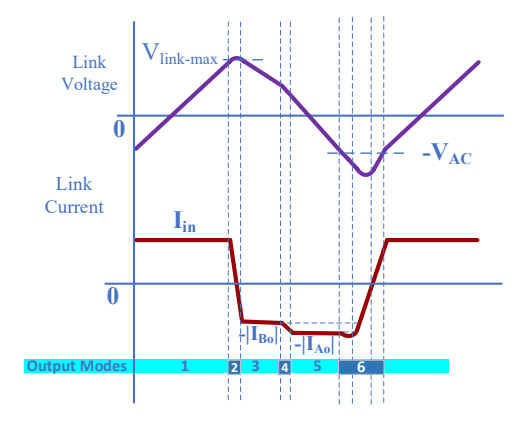


Fig. 5. Voltage and current waveforms of the link capacitor in the Zeta-based AC-AC converter.

In the last resonating mode  $L_{resonance}$  and  $C_{link}$  resonate until the link current becomes equal to the input inductor current ( $I_{in}$ ) to help turn off  $Q_1$  and  $Q_6$  under ZCS (Fig. 6(h)).

It should be noted that the input inductor charging modes are similar to what was discussed in Part (A) for the Zeta-based rectifier and are controlled independently with the link discharging modes and resonating modes.

#### III. SIMULATION AND EXPERIMENTAL RESULTS

This section presents simulation and experimental results corresponding to the Zeta rectifier, Zeta-based AC-AC converter, and the Zeta inverter to validate the performance of the proposed universal converter. The parameters of the converter specific to each case are summarized in Table I.

# A. Zeta Rectifier

Figures 7-10 represent the simulation results obtained for the proposed soft-switching Zeta rectifier. In Fig. 7, the voltage and

current waveforms for the link capacitor are depicted, highlighting the capability of the converter to allow for a negative link voltage during a small portion of time. This feature enables the utilization of a small capacitor with a lower voltage rating compared to Ćuk-based universal converters. Fig. 8 illustrates the input inductor voltage and current. The unfiltered input currents and the voltage and current waveforms of one of the switches, which verifies zero current turn off and soft turnon, are shown in Fig. 9. Fig. 10 demonstrates the DC voltage and the filtered three-phase input currents with a THD of 2.5%.

## B. Zeta-based AC-AC Converter

Simulation results corresponding to the designed softswitching Zeta-based AC-AC converter are illustrated in Figs. 11-15. The voltage and current of the link capacitor and input inductor are given in Figs. 11 and 12, respectively. Similar to the Zeta rectifier, the minimum value of the link voltage can be negative to reduce the link peak voltage compared to Cuk-based AC-AC converters. Fig. 13 illustrates the unfiltered three-phase output voltages and input currents. The voltage and current waveforms of one of the input and output switches are shown in Fig. 14 to verify the zero current turn off and soft turn-on of the switches in this converter. Fig. 15 shows the output three-phase filtered voltages with a THD of 2%, and the three-phase filtered input currents with a THD of 2.5%.

# C. Zeta Inverter

A prototype of the proposed universal converter was fabricated and used to evaluate its performance, as shown in Fig. 16. Experimental results for the three-phase Zeta inverter are presented in Fig. 17-20. Figs. 17 and 18 display the voltage and current waveforms for the link capacitor and the input inductor, respectively. The unfiltered output voltages with two different discharging modes are represented in Fig. 19. Finally, Fig. 20 shows the filtered input DC current and the filtered output three-phase voltages with a unity power factor.

TABLE I. ZETA-BASED UNIVERSAL CONVERTER PARAMETERS

	Link frequency	Link capacitance	Input inductance	Power level	Input line-to-line three-phase or DC Voltage amplitude	Output line-to-line three-phase or DC Voltage amplitude
Rectifier	30 kHz	200 nF	200 uH	2 kW	200 V	275 V
AC-AC converter	30 kHz	200 nF	500 uH	1 kW	200 V	190 V
Inverter	5 kHz	2 uF	500 uH	1 kW	90 V	110 V

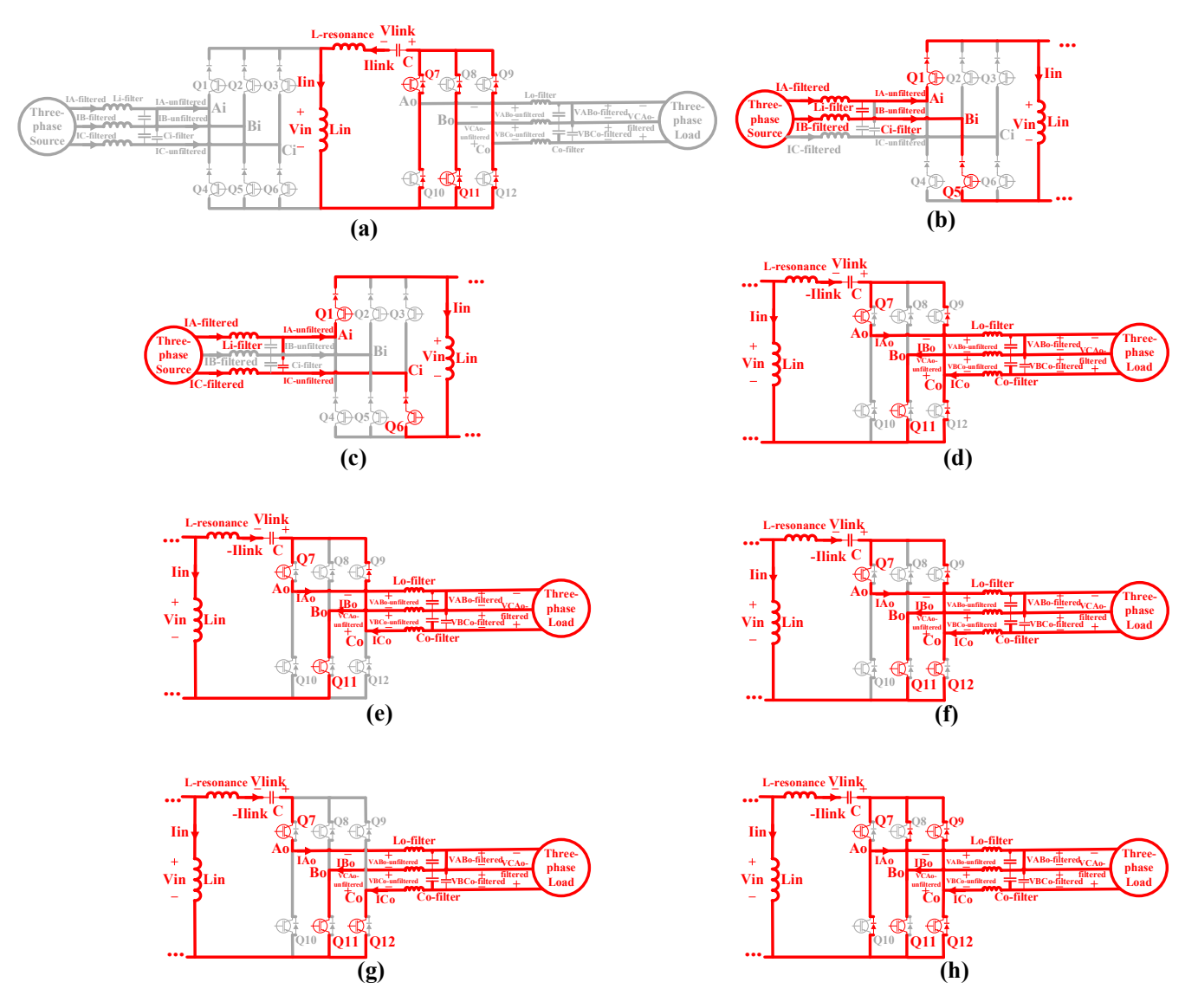


Fig. 6. Behavior of the non-isolated soft-switching three-phase AC-AC Zeta converter during: (a) mode 1, (b) first inductor charging mode (input mode 2), (c) second inductor charging mode (input mode3), (d) first resonating mode (output mode 2), (e) first capacitor discharging mode (output mode 3), (f) second resonating mode (output mode 4), (g) second capacitor discharging mode (output mode 5), (h) third resonating mode (output mode 6).

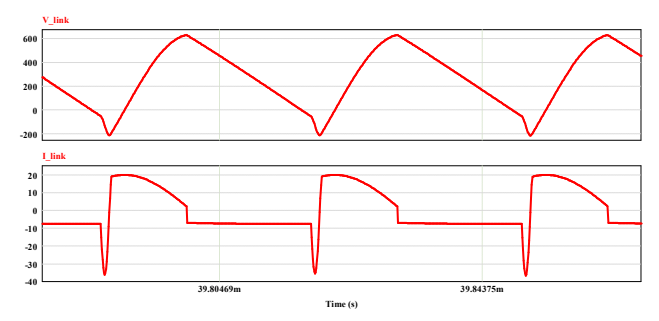


Fig. 7. Link capacitor voltage and current waveforms in the Zeta rectifier (simulation).

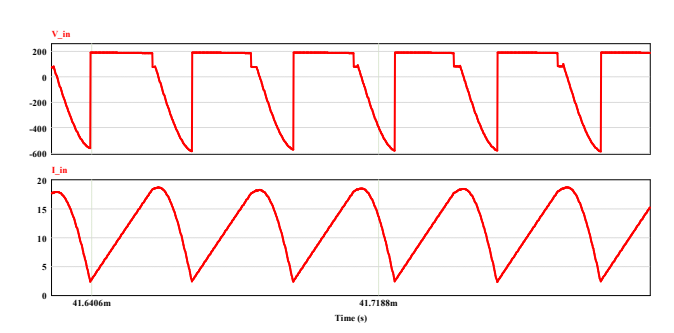


Fig. 8. Input inductor voltage and current waveforms in the Zeta rectifier (simulation).

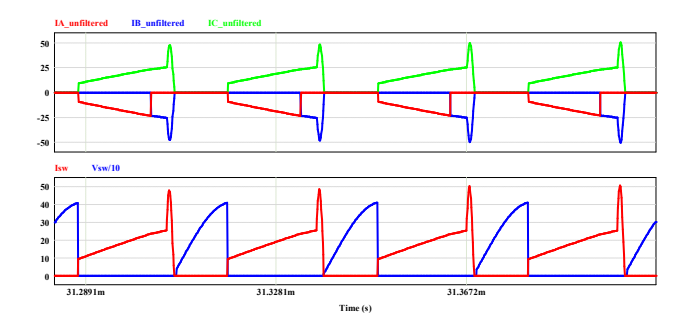


Fig. 9. Three-phase unfiltered input currents, and the scaled voltage and current waveforms of one of the switches in the Zeta rectifier (simulation).

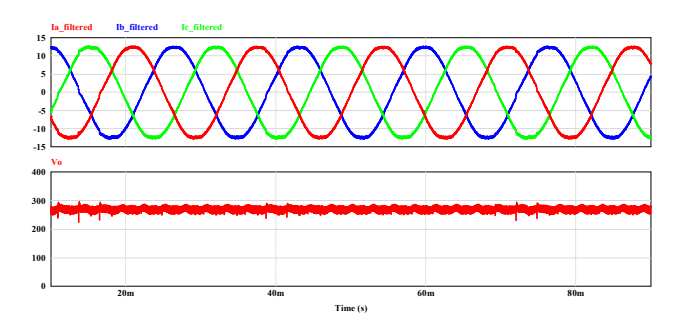


Fig. 10. Three-phase filtered input currents and output DC voltage in Zeta rectifier (simulation).

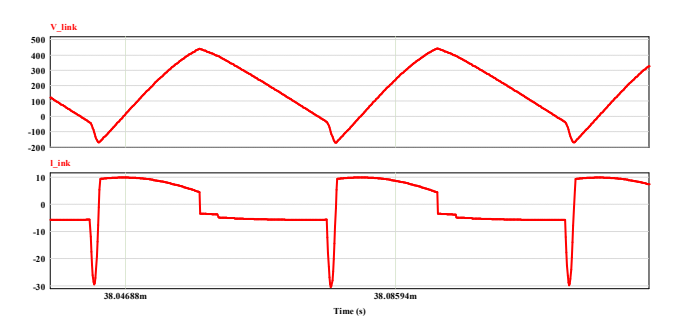


Fig. 11. Link capacitor voltage and current waveforms in Zeta-based AC/AC converter (simulation).

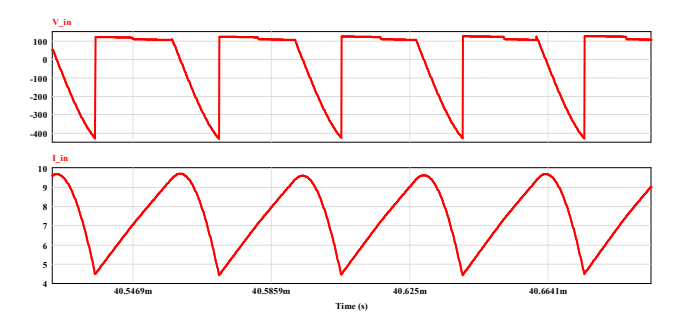


Fig. 12. Input inductor voltage and current waveforms in Zeta-based AC/AC converter (simulation).

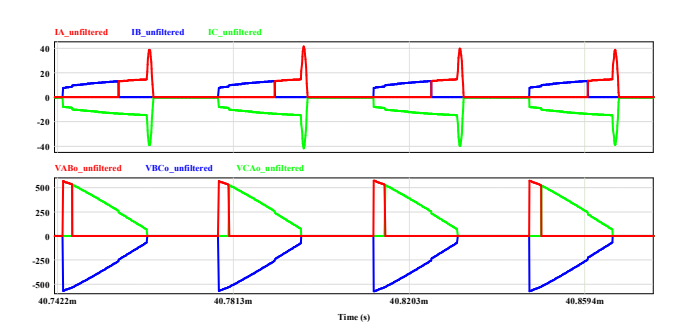


Fig. 13. Three-phase unfiltered input currents and three-phase unfiltered output voltages in Zeta-based AC/AC converter (simulation).

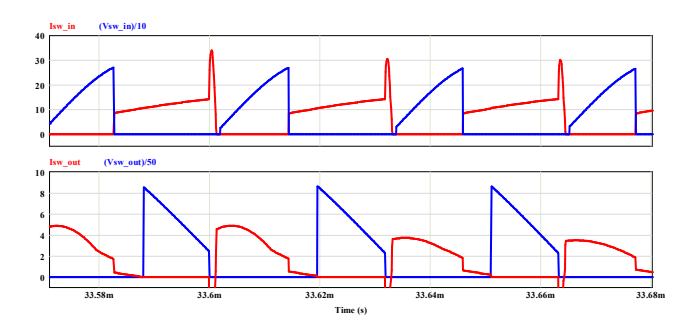


Fig. 14. The scaled voltage and current waveforms of the input and output switches in Zeta-based AC/AC converter (simulation)

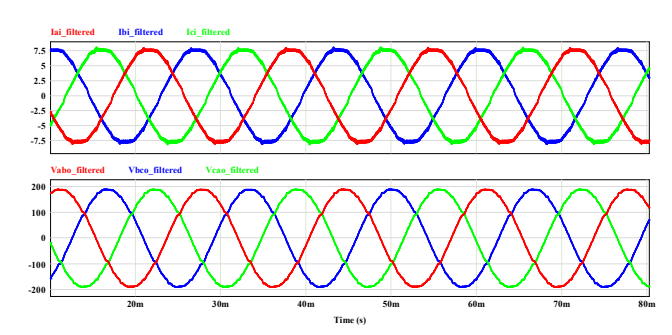


Fig. 15. Three-phase filtered input currents and three-phase filtered output voltages in Zeta-based AC/AC converter (simulation).



Fig. 16. Experimental Setup.

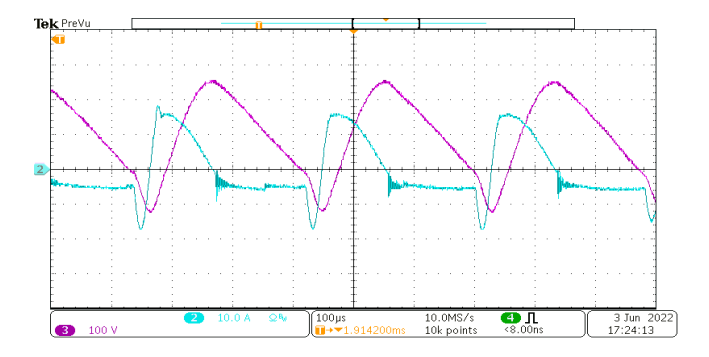


Fig. 17. Link current and voltage for the Zeta inverter (Experimental).

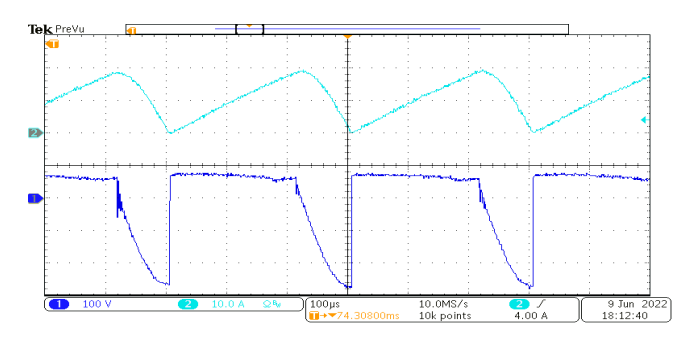


Fig. 18. Input inductor current and voltage for the Zeta inverter (Experimental).

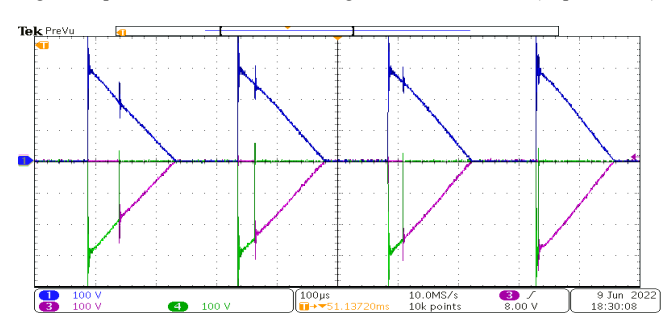


Fig. 19. Unfiltered three-phase voltages for the Zeta inverter (Experimental).

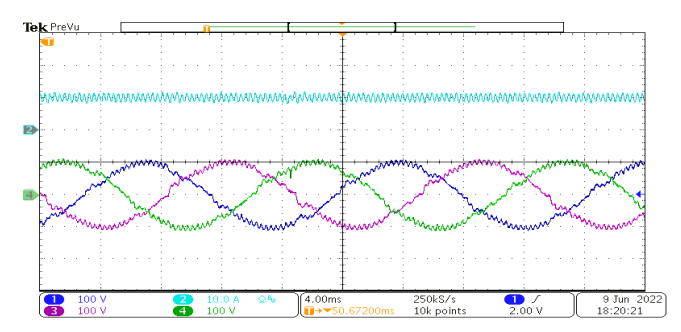


Fig. 20. Filtered DC input current and filtered three-phase voltages for the Zeta inverter (Experimental).

### IV. CONCLUSION

This paper presented a soft-switching Zeta-based universal converter that can be used as a rectifier, an AC-AC converter, or a three-phase inverter. Due to the elimination of the bulky electrolytic capacitors and the low-frequency transformers, the size and weight of the proposed converter are expected to be lower than traditional DC-link universal converters. Furthermore, compared to Ćuk-based universal converters, this topology has a lower link peak voltage. In this topology, the switches benefit from zero current turn-off and soft turn-on.

#### ACKNOWLEDGMENT

This material is based upon work supported by the National Science Foundation under Grant No. 2047213.

#### REFERENCES

- [1] C.-J. Shin and J.-Y. Lee, "An electrolytic capacitor-less bi-directional EV on-board charger using harmonic modulation technique," *IEEE Trans. Power Electron.*, vol. 29, no. 10, pp. 5195 – 5203, Oct. 2013.
- [2] H. Wang and F. Blaabjerg, "Reliability of capacitors for DC-link applications in power electronic converters—An overview," *IEEE Trans. Ind. Appl.*, vol. 50, no. 5, pp. 3569 – 3578, Sep./Oct. 2014.
- [3] T. Friedli, J. W. Kolar, J. Rodriguez, and P. W. Wheeler, "Comparative evaluation of three-phase AC-AC matrix converter and voltage DC-link back-to-back converter systems," *IEEE Trans. Ind. Electron.*, vol. 59, no. 12, pp. 4487 – 4510, Dec. 2012.
- [4] L. Kim and G. Cho, "New bilateral zero voltage switching AC/AC converter using high frequency partial-resonant link," in 16th Annual Conference of IEEE Industrial Electronics Society, 1990, pp. 857-862.
- [5] M. Amirabadi, J. Baek, H. A. Toliyat, and W. C. Alexander, "Soft-Switching AC-Link Three-Phase AC-AC Buck-Boost Converter," *IEEE Transactions on Industrial Electronics*, vol. 62, no. 1, pp. 3-14, 2015.
- [6] K. Mozaffari and M. Amirabadi, "A Highly Reliable and Efficient Class of Single-Stage High-Frequency AC-Link Converters," in IEEE Transactions on Power Electronics, vol. 34, no. 9, pp. 8435-8452, Sept. 2019, doi: 10.1109/TPEL.2018.2888583.
- [7] E. Afshari, M. Khodabandeh and M. Amirabadi, "A Single-Stage Capacitive AC-Link AC-AC Power Converter," in IEEE Transactions on Power Electronics, vol. 34, no. 3, pp. 2104-2118, March 2019, doi: 10.1109/TPEL.2018.2841398.
- [8] M. Khodabandeh, E. Afshari, and M. Amirabadi, "A Single-Stage Soft-Switching High-Frequency AC-Link PV Inverter: Design, Analysis, and Evaluation of Si-Based and SiC-Based Prototypes," *IEEE Transactions on Power Electronics*, vol. 34, no. 3, pp. 2312-2326, 2018.
- [9] M. Khodabandeh and M. Amirabadi, "A Soft-switching Single-stage Zeta-/SEPIC-based Inverter/Rectifier," 2020 IEEE Applied Power Electronics Conference and Exposition (APEC).
- [10] M. Salehi, M. Khodabandeh and M. Amirabadi, "Zeta-Based AC-Link Universal Converter," 2022 IEEE Energy Conversion Congress and Exposition (ECCE), 2022, pp. 1-7, doi: 10.1109/ECCE50734.2022.9947744.
- [11] M. Salehi and M. Amirabadi, "A Soft-Switching Zeta-Based AC-Link Universal Converter," 2023 IEEE Applied Power Electronics Conference and Exposition (APEC), Orlando, FL, USA, 2023, pp. 3233-3239, doi: 10.1109/APEC43580.2023.10131175.